$(V_2O_5)_n$ Gas-Phase Clusters ($n = 1-12$) Compared to V_2O_5 Crystal: DFT Calculations

Sergei F. Vyboishchikov and Joachim Sauer*

Humboldt-Universität zu Berlin, Institut für Chemie, Arbeitsgruppe Quantenchemie, Jägerstr.10-11, D-10117 Berlin, Germany

Received: June 18, 2001

Stable structures of neutral $(V_2O_5)_n$ clusters ($n = 1-5$, 8, 10, and 12) are determined by density functional calculations (BP86 functional with a double-ζ (V)/triple-ζ (O) valence basis set augmented by polarization functions). Comparison is made with calculations for the periodic structure of solid V_2O_5. The most stable structure of the smallest cluster is doubly O-bridged, $OV-O_2-VO_2$, and by 184 kJ/mol $VO_{2.5}$ less stable than the periodic bulk structure. From the tetrahedral V_4O_{10} structure on (41 kJ/mol $VO_{2.5}$ above the crystal energy) polyhedral cage structures are the most stable isomers: trigonal prism (V_6O_{12}), cube (V_8O_{20}), pentagonal prism ($V_{10}O_{25}$), 16-hedron ($V_{16}O_{40}$), dodecahedron ($V_{20}O_{50}$), and truncated octahedron ($V_{24}O_{60}$). The polyhedra have vanadyl groups at the apexes and bridging oxygen atoms on the edges. Differently from the crystal structure, vanadium is 4-fold coordinated and 3-fold coordinated oxygen is avoided. The energies relative to the periodic solid are 22.1, 12.4, 9.4, 5.5, 3.3, and 3.4 kJ/mol $VO_{2.5}$, respectively. Structures that correspond to fragments cut out of the crystal structure (examined up to $n = 8$) are significantly less stable. The IR spectra of cage-type structures will show bands in the 1040−1080 cm^{-1} and in the 800−925 cm^{-1} regions (terminal $V{=}O^{(1)}$ and bridging $V-O^{(2)}-V$, respectively), but not between 650 and 750 cm^{-1} or around 500 cm^{-1} ($V-O_2^{(2)}-V$ double bridges and triply coordinated oxygen, respectively).

1. Introduction

How structure, properties, and reactivity of a chemical compound change when passing from small molecules over nanosized clusters to the bulk solid, belongs to the fundamental questions in understanding materials. While in the 1960s and early 1970s cluster studies mainly dealt with metals,[1] more recently the interest has expanded to metal oxides, e.g., magnesium,[1] titanium,[2] niobium,[3] and zirconium[4] oxides. Mass spectrometry yields cluster size distributions and renders reactivity studies possible, whereas characterization of cluster structures remains a challenge for experimentalists. Even if infrared spectra of metal oxide clusters become available, their assignment to specific cluster structures requires assistance by quantum mechanical calculations as a study on Zr_nO_{2n-1} clusters shows.[4] The emergence of bulk-type structural properties with size is of prime interest. Already small $(NaCl)_n$, $(KCl)_n$, and $(LiF)_n$ clusters adopt cubic structures typical of the periodic crystal structures,[5−7] while for alkaline earth oxides the critical cluster size where anions with bulk coordination first appear is much larger (See ref 8 and references therein).

This study deals with divanadium pentaoxide and we address the question how the structures of small to nanosize gas-phase clusters of V_2O_5 differ from that of the bulk solid. Our interest in this material arises from its important use as solid oxidation catalyst,[9−11] specifically from the fact that many active catalysts contain vanadium oxide highly dispersed on different supports. While the crystal structure of solid V_2O_5 is well-described,[12] nothing is known about the structure of the V_2O_5 molecule or larger $(V_2O_5)_n$ clusters. Experimentally, mostly charged gas-phase vanadium oxide species were studied, since they are much easier to separate and to identify by mass spectrometric techniques than neutral species (see refs 13−17 for cations and refs 18−21 for anions). Foltin et al.[22] studied the growth dynamics of neutral V_xO_y clusters obtained by laser ablation of vanadium metal in the presence of oxygen. Previously we reported the structures of mono- and polynuclear vanadium oxide anions[23] and made predictions of vertical detachment energies and of adiabatic electron affinities of the respective neutral species.

Here, we employ density functional methods to predict the structure and stability of $(V_2O_5)_n$ gas-phase clusters ($n = 1-12$) and compare them with the crystal structure of the bulk solid V_2O_5. For this purpose, calculations on the periodic structure of divanadium pentaoxide were performed at the same computational level although calculations applying periodic boundary conditions have been made before using various techniques.[24−32] Solid V_2O_5 has a layered structure[12] shown in Figure 1. The layers are made up of double ribbons that stretch along the crystal *B* axis and, in *A* direction, are connected by oxygen bridges. Vanadium atoms are pentacoordinated within a layer, with an additional weak interlayer bond, resulting in a 6-fold coordination. There are three different types of oxygen atoms: mono-coordinated oxygen atoms within the vanadyl groups, doubly coordinated oxygen atoms that form bridges between the ribbons, and triply coordinated oxygen atoms within one ribbon. We show that the coordination is different in the most stable isomers of the $(V_2O_5)_n$ clusters ($n = 1-12$) which have a polyhedral structure. Vanadium is always four-coordinated, and oxygen is mono-coordinated within vanadyl groups or two-coordinated as bridge between $V{=}O(O-)_{3/2}$ pyramids. Inspite of this different coordination pattern, the stability of the largest of the clusters is only marginally smaller than that of the bulk crystalline solid (a few kJ/mol $VO_{2.5}$).

* To whom correspondence should be addressed. Address: Humboldt-Universität zu Berlin, Arbeitsgruppe Quantenchemie, Jägerstrasse 10-11, D-10117 Berlin, Germany. Fax: +49-30-20192302. E-mail: js@qc.ag-berlin.mpg.de.

10.1021/jp012294w CCC: $20.00
Published on Web 08/24/2001

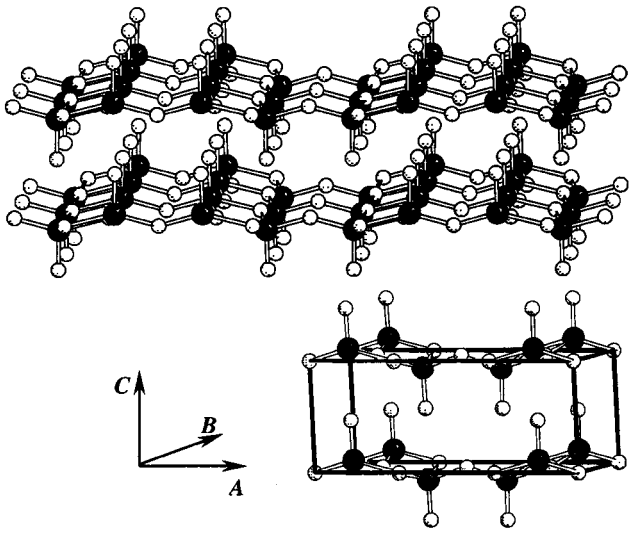

Figure 1. Structure of crystalline divanadium pentaoxide.

2. Computations

2.1. Methods Used. We employ density functional (DF) techniques[33] and make use of two different functionals: (1) B3LYP,[34,35]a hybrid functional combining Becke's 1988 nonlocal exchange[36] with Hartree−Fock exchange along with the Lee−Yang−Parr[37] correlation functional, and (2) BP86,[38] Becke's exchange functional[36] in combination with Perdew's correlation functional. For transition metal complexes, the B3LYP functional yields accurate structures and, in many cases, also reasonable relative energies.[39,40] The BP86 functional, even if generally less reliable, performs well (particularly for geometries) for many systems including some transition metal compounds,[41] and permits substantial savings of computation time when the RI-DFT ("resolution of identity") procedure[42] is applied.

The calculations were performed with all-electron double-ζ and triple-ζ valence basis sets developed by Ahlrichs and coworkers[43] augmented by a set of polarization functions (a p-set for vanadium, a d-set for oxygen).[44] Table 1 shows basis sets tested for the purpose of the present study. Calculations on V_2O_5 showed that on vanadium the TZVP basis can be safely replaced by DZVP, e.g. the energy difference between two different configurations of V_2O_5 (singly and doubly bridged ones, vide infra) changes by less than 1 kJ/mol. This mixed basis set, which is TZVP for oxygen and DZVP for vanadium, was employed throughout the study and is referred to as D(T)ZVP. The idea behind using such a basis set is that oxygen atoms, which are negatively charged in oxides, need a more flexible basis set than the electron-deficient metal atoms.

To confirm the nature of stationary points found by optimization, calculations of harmonic force constants were carried out for all the clusters of V_2O_5 and V_4O_{10} composition, as well as for the cage-type V_6O_{15} and V_8O_{20} clusters at the BP86/D(T)-ZVP level using the Gaussian 94 package.[45] For larger clusters, frequency calculations are not affordable on routine basis. To strengthen confidence that minima rather than saddle points are found, the optimizations were made either without symmetry constraints, or, when a minimum was found under symmetry constraints, it was distorted to destroy the symmetry and reoptimized. If this procedure did not result in an energy gain, the symmetric structure was accepted. All geometry optimizations were performed with the TURBOMOLE program package.[46−48]

2.2. Performance of the Methods. To test the performance of the computational method chosen, calculations have been made with the TZVP basis on small vanadium-containing molecules, for which experimental gas-phase data is available.[23] For the calculated structures, both functionals give a very good agreement with the experiment. Bond distances differ by at most 3 pm, B3LYP doing slightly better. Comparison between the experimental and calculated atomization energies shows that B3LYP/TZVP typically underestimates the atomization energies, whereas the BP86/TZVP results are in excellent agreement with the experiment. For the energy difference between the two V_2O_5 structures (Table 1), BP86 yields a larger value (77.4 kJ/mol) than B3LYP (69.7 kJ/mol).

Moreover, we optimized two vanadium(V) complexes for which X-ray structures are available. One of them is $VO(OC_6H_3Pr^i_2\text{-}2,6)_3$.[49] Both B3LYP and BP86 functionals with the D(T)ZVP basis set yield a C_{3v} structure with a tetrahedrally coordinated central vanadium atom for the model compound triphenylvanadate $VO(OPh)_3$ shown in Figure 2a. The bond lengths calculated at the B3LYP/D(T)ZVP level differ from the experimental results by at most 1.3 pm. The deviation of the BP86 structure from the experiment is slightly larger, but the accordance is still rather good (within 2 pm).

The second example is dimeric trimethylvanadate $(VO(OMe)_3)_2$.[50,51] It contains two pentacoordinated tetragonal−pyramidal vanadium atoms connected through two MeO bridges (Figure 2b). The coordination of the vanadium atoms resembles that in solid V_2O_5. Similarly to the solid V_2O_5 structure, there are three distinct types of oxygen atoms: terminal with a V−O distance of about 160 pm, doubly coordinated with a V−O distance of about 180 pm, and triply coordinated bridging oxygen atoms with a V−O distance of about 200 pm. The structure optimized using the B3LYP and BP86 functionals with the D(T)ZVP basis set has C_2 symmetry (Figure 2b). For the $V-O^{terminal}$ bond length, the B3LYP result virtually coincides with the experimental value. For the $V-O^{Me-bridging}$ bond, B3LYP and experimental distances are also in good agreement with each other. For the nonbridging V−O bonds, B3LYP yields two rather similar values (178 and 179 pm), while the X-ray distances show a larger variation (174 and 186 pm). The average (180 pm) is again close to the B3LYP result. This shows that the splitting observed by X-ray may well be due to crystal

TABLE 1: Basis Set Used in the Present Work and Number of Basis Functions (no. of BF) per $VO_{2.5}$ unit

					$E(C_2)-E(C_s)^a$	
basis set	description	contraction scheme {s/p/d} functions	(no. of BF)	refs	B3LYP	BP86
DZP	double-ζ + polarization functions	V: {62111111/331111/311} O: {5111/31/1}	78.5	67	83.7	95.8
TZVP	TZV + polarization functions	V: {842111/6311/411} O: {62111/411/1}	80.5	43, 44	69.0	78.2
D(T)ZVP		V: {63311/531/41} O: {62111/411/1}	71.5	43	69.7	77.4

[a] Energy difference between the singly and doubly bridged configurations of the V_2O_5 molecule, $E(C_2) - E(C_s)$, in kJ/mol $VO_{2.5}$. The doubly bridged $OV-O_2-VO_2$ structure is more stable.

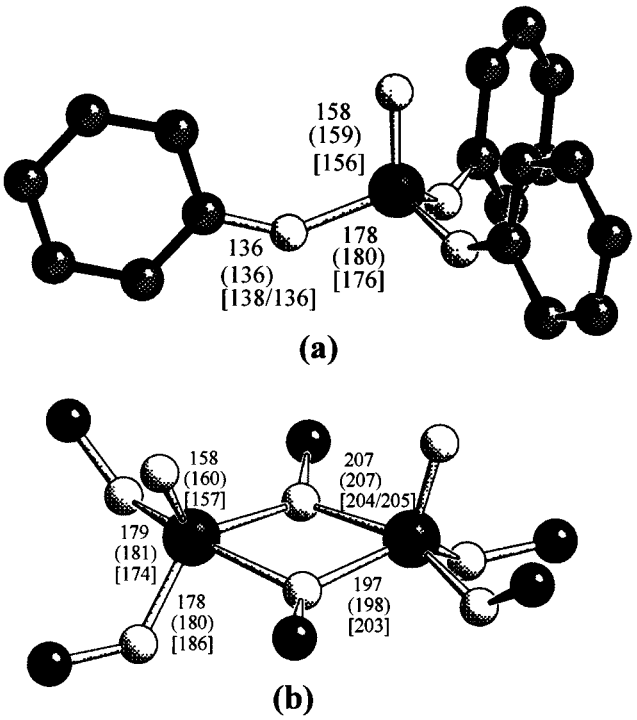

Figure 2. DFT/D(T)ZVP optimized structures of $OV(OPh)_3$ (**a**) and $(OV(OMe)_3)_2$ (**b**). B3LYP results without brackets, BP86 results in parentheses "()", experimental values in brackets "[]". Hydrogen atoms are omitted for clarity.

packing effects (weak dimeric interaction between two $(VO(OMe)_3)_2$ molecules). Hence, the overall agreement of the B3LYP/D(T)ZVP distances with the experimental results is considered satisfactory. The BP86 distances differ by at most 2 pm from the B3LYP ones. Both in $(VO(OMe)_3)_2$ and in $VO(OPh)_3$, BP86 generally yields slightly longer bond lengths than B3LYP.

2.3. Solid-State Calculations. For the periodic calculation the CRYSTAL-95 code[52] was employed. Comparison of gas-phase clusters and bulk solids is only meaningful if the same Gaussian basis sets are used for both calculations. When working with the original D(T)ZVP basis set, the two outermost s-functions for vanadium ($\zeta = 0.072$ and 0.027) cause a basis set linear dependency at reasonable integration cutoffs. To overcome this problem, we reoptimized these two exponents by minimization of the BP86 crystal energy at the experimental bulk structure[53]and obtained $\zeta = 0.348$ and $\zeta = 0.166$ for the outermost functions. Catti et al.[54] obtained values of $\zeta = 1.04$ and $\zeta = 0.4346$ by completely optimizing an 8−411G*-type basis set for V_2O_3. Though these values differ by about a factor of 3 from ours, the general trend is that the optimum exponents for a solid are much less diffuse that those for an atom. We will refer to the basis set as D(T)ZVP′. This basis set was used for the crystal structure optimization, whereas the cluster calculations employed the original Ahlrichs's basis sets.[43] To assess the performance of the "solid state" basis sets for the clusters calculations, we reoptimized the structure of the V_2O_5 and V_4O_{10} clusters using the D(T)ZVP′ basis set. The bond length show a maximum difference of 0.5 pm. The total energy obtained with the modified basis set D(T)ZVP′ is lower by 11.0−12.5 kJ/mol $VO_{2.5}$ than that obtained with the original basis set (Table 2). However, the relative stabilities of the different species change by at most 1.5 kJ/mol $VO_{2.5}$.

Since analytical energy gradients are not implemented in CRYSTAL-95, the crystal V_2O_5 structure was optimized using numerical gradients. The gradients were calculated by a two-point formula with step size of 0.2 pm for unit cell parameters and 0.0001 or 0.0002 for fractional atom coordinates. Unit cell parameters and fractional atom coordinates were optimized simultaneously using the quasi Newton−Raphson method and BFGS Hessian update with a simple five-point line search. The optimization was stopped when the maximum component of the gradient did not exceed 0.01 hartree/Å. The experimentally found *Pmmn* space group was kept during the optimization. A total of 27 points of the reciprocal unit cell (including equivalent ones) were used in the course of optimization, whereas for the final energy evaluation up to 405 *k* points were used.

TABLE 2: Absolute Energy Difference between BP86/D(T)ZVP′ and BP86/D(T)ZVP Optimized Structures[a]

molecule	ΔE, kJ/mol $VO_{2.5}$
V_4O_{10}	
TETRA	12.2
SQUARE	11.3
DOUBLE-BRIDGE	12.5
CHAIN	11.7
RIBBON	11.0
V_2O_5	
$VO-O_2-VO_2$	11.2
VO_2-O-VO_2	12.2

[a] The D(T)ZVP′ energies are always lower.

TABLE 3: Experimental and Calculated Unit Cell Parameters and Fractional Coordinates for Solid V_2O_5, as Well as Selected Interatomic Distances

	experiment[53]			BP86/D(T)ZVP′		
	A	B	*C*	*A*	B	C
	11.512	3.564	4.368	11.74	3.56	4.47
	x	y	*z*	*x*	y	z
V	0.1012	0.25	0.8917(2)	0.1042	0.25	0.8835
O1	0.1043	0.25	0.531(1)	0.1062	0.25	0.5273
O2	−0.0689	0.25	0.003(1)	−0.0681	0.25	0.0236
O3	0.25	0.25	0.001(2)	0.25	0.25	−0.0029
V−O1	1.576			1.592		
V−O2	1.778			1.786		
V−O3	1.878			1.875		
V−O4	2.017			2.117		
V···O	2.793			2.877		

3. V_2O_5 Bulk Structure

Solid V_2O_5 belongs to the orthorhombic crystal system (space group *Pmmn*) and has four V_2O_5 formula units per unit cell (Figure 1).[12] Table 3 shows the BP86/D(T)ZVP′ results for bulk V_2O_5. Comparison with the experimental values indicates that the DFT calculation reasonably reproduces both the cell parameters (within 2%) and the atomic coordinates. For three different V−O bonds within one V_2O_5 layer, the calculated interatomic distances agree with the respective experimental ones within 2 pm. The longest of the three $V-O^{triply}$ bonds, V−O4, and the interlayer V···O distance are too long by 10 and 8 pm, respectively. The latter is essentially of intermolecular character, and a proper description may therefore be a challenge for DFT calculations. Overall, the quality of the structure obtained is satisfactory. Under periodic boundary conditions the periodic bulk structure of V_2O_5 was previously optimized by Kempf et al.[24] who applied the Hartree−Fock method, and by Yin et al.[32] using DFT (LDA- and GGA-based functionals). Augmented spherical wave calculations [29,30] within the LDA approach have also been reported. Most recently, the full potential linearized augmented plane wave method in conjunction with the LDA functional was used by Chakrabarti et al.[31]

TABLE 4: Relative Energies of $(V_2O_5)_n$ Clusters in kJ/mol $VO_{2.5}$ with Respect to the Crystalline Divanadium Pentaoxide[a]

			relative energy	
2*n*	molecule	point group	B3LYP	BP86
2	**2-SINGLE BRIDGE**	C_2	223.5	223.1
	2-DOUBLE-BRIDGE	C_s	188.7	184.3
4	**4-SINGLE-BRIDGE**	C_1	143.7	138.0
	4-DOUBLE-BRIDGE	C_i	130.6	131.4
	4-RIBBON	C_i	112.2	113.6
	4-CHAIN	D_{2h}	102.3	100.2
	4-SQUARE	D_{2h}	56.3	56.1
8	**8-POLYCYCLE−2**	C_2		97.9
	8-POLYCYCLE−1	C_1		78.6
	8-SHEET-2	C_s		77.8
	8-SHEET-1	C_1		70.1
	8-SHEET-4	C_s		64.8
	8-SHEET-3	C_1		64.0
	8-SHEET-5	C_s		61.0
	8-RIBBON	C_i		57.0
	8-TWO-LAYER-1	C_1		52.7
	8-TWO-LAYER-2	C_1		39.1
16	**16-DOUBLE RIBBON**	C_1		60.8
	16-SHEET	C_1		46.9
	16-TWO-LAYER	C_1		15.3
∞	bulk crystal	*Pmmn*		0.0

[a] The relative B3LYP values are obtained by extrapolation assuming equal B3LYP and BP86 relative energies for the V_4O_{10} **TETRA** cluster.

for partial structure optimizations of the three-dimensional structure (bulk) and of a single layer (slab model). The resulting bulk structure is in very good accord with the experiment. The Cartesian atomic coordinates agree up to about 0.01 Å, and the unit cell parameters are underestimated by ∼1.25% only. The optimized one-layer structure differs very little from that of the bulk.

To estimate the strength of the interaction between the individual layers in the crystal, we calculated the energy of a single layer using the SLAB option of the CRYSTAL program[52] (interlayer distance 500 Å, experimental intralayer structure). The resulting absolute energy per unit cell is 9.8 kJ/mol higher than for the bulk crystal. Thus, the layer interaction energy per $VO_{2.5}$ unit is as low as 2.5 kJ/mol. Yin et al.[32] reported an estimate of about 4.2 kJ/mol $VO_{2.5}$. Despite the uncertainty of these results due to the limited performance of DFT for weak bonds, and of a possible basis set superposition error, the conclusion is reached that the interaction between the V_2O_5 layers is very weak, of the order of few kJ/mol $VO_{2.5}$.

4. $(V_2O_5)_n$ Gas-Phase Cluster

In this section we examine the structures and stabilities of $(V_2O_5)_n$ clusters for $n = 1-12$. The smaller clusters, V_2O_5 and V_4O_{10}, were studied systematically, so that all or nearly all low-energy structures are included. For the larger clusters, V_8O_{20} and $V_{16}O_{40}$, only selected structures were considered. The initial structures are either fragments cut out from the V_2O_5 crystal structure ("analytic" approach), or designed according to building principles found for the smaller clusters ("synthetic" approach). In addition, two selected examples of medium-size clusters, V_6O_{15} and $V_{10}O_{25}$, as well as two big clusters, $V_{20}O_{50}$ and $V_{24}O_{60}$, are discussed. Tables 4 and 5 show the relative energies. The optimized bond distances and angles for V_2O_5 clusters are given in Table 6. For bigger clusters, only average bond length of different types are summarized in Table 7. Comparison of observed and calculated bond lengths indicates that $V-O^{(1)}$ and $V-O^{(2)}$ distances are overestimated by 1 pm.

4.1. V_2O_5 Clusters. As already mentioned in our previous paper,[23] three configurations of the V_2O_5 molecule are conceivable: with one, two, or three bridging oxygen atoms (cf. Figure 3). The latter structure, $OV-(O)_3-VO$, with C_{3v} symmetry was found to be a higher order saddle point on the potential energy surface (PES). Its optimization without symmetry constraints results in the doubly bridged O_2V-O_2-VO configuration (C_s symmetry), which is by 77 kJ/mol more stable than the singly bridged one (C_2 symmetry).

The doubly bridged O_2V-O_2-VO molecule has one tetracoordinated (V1) and one triply coordinated (V6) vanadium atom. The latter has a pseudotetrahedral coordination with one vacant position. Assuming that the three terminal V═O bonds with distances between 159 and 160 pm are double bonds, the valence of 5 for V and the valence of 2 for O implies bond orders of 1.5 for the V6−O5 and V6−O4 bonds having distances of about 170 pm and bond orders of 0.5 for the V1−O4 and V1−O5 bonds. The latter are almost 200 pm long, i.e., this bond order scheme is supported by the calculated bond distances.

In the singly bridged V_2O_5 structure the VO_3 units are slightly pyramidal, the sum of the O−V−O angles being 346° and 339°

TABLE 5: Relative Energies of $(V_2O_5)_n$ Clusters with Spherical Shape (cages) in with Respect to the Crystalline Divanadium Pentaoxide (kJ/mol $VO_{2.5}$)[a]

2*n*	molecule	faces[a]	point group	relative energy BP86
4	**TETRAhedron**	3^4	T_d	41.0
6	**TRIgonal PRISM**	4^33^2	C_1	22.1
8	**CUBE**	4^6	S_4	12.4
10	**PENTAgonal PRISM**	4^55^2	C_1	9.4
16	**OCTAgonal PRISM**	4^88^2	C_1	7.6
16	**16-hedron**	5^84^2	C_1	5.5
20	**DODECAhedron**	5^{12}	D_{3d}	3.3
24	**TRUNCated OCTAhedron**	6^84^6	T_d	3.4
∞	bulk solid			0.0

[a] We use notation m^k, where k is the number of m-gons defining the faces. $\sum k$ is equal to the number of faces of the polyhedron.

TABLE 6: Calculated Interatomic Distances (at B3LYP/D(T)ZVP Level and BP86/D(T)ZVP Level, in Picometers) and Bond Angles (in Degrees) in the V_2O_5 clusters

molecule	parameter	B3LYP	BP86
$VO-O_2-VO_2$	V6−O7	157.9	159.5
	V1−O2	158.3	159.9
	V1−O3	158.7	160.3
	V6−O4	169.0	170.4
	V1−O4	199.4	198.9
	∠V1−O4−V6	93.9	93.3
	∠O2−V1−O3	111.0	110.9
	∠O2−V1−O4	118.3	118.3
VO_2-O-VO_2	V1−O5	158.6	160.7
	V1−O4	158.8	160.9
	V1−O3	179.7	180.3
	∠O3−V1−O5	118.1	116.5
	∠O4−V1−O5	111.0	110.1

TABLE 7: Comparison of Experimental and Calculated (BP86/D(T)ZVP) Bond Lengths in Picometers in $(V_2O_5)_n$ Clusters, Bulk V_2O_5 Solid, and Bis(trimethoxyvanadate) $(VO(OMe)_3)_2$

		V═O	$V-O^{(2)}$	$V-O^{(3)}$
$(VO(OMe)_3)_2$	obsd	158	179[a]	203
	calcd	159.3	180.3[a]	202.5[a]
bulk solid	obsd	157.6	177.8	187.8; 201.7
	calcd	159.2	178.6	187.5; 211.7
all clusters	from−to	155.1−162.4	164.4−212.0	176.8−217.0
	average	158.6	179.7	194.4
cage-type clusters	from−to	157.0−160.3	170.4−198.9	
	average	158.2	178.6	

[a] Average of two different values.

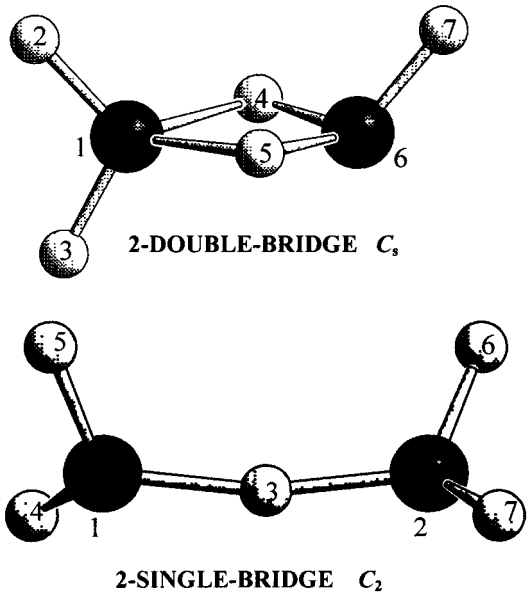

Figure 3. DFT optimized structures of two isomers of the V_2O_5 molecule.

for the B3LYP and BP86 functionals, respectively. However, this pyramidalization is much smaller than that of the V6 atom in the doubly bridged molecule (322° and 320°, respectively).

4.2. V_4O_{10} Clusters. First, we consider V_4O_{10} units cut out from the crystal structure of V_2O_5 in various ways ("analytic approach"). The **4-ONE-BRIDGE** cluster (Figure 4) is obtained by optimization of a V_4O_{10} fragment cut from two neighboring ribbons of the crystal along the *A* crystal axis. The structure is strongly dissymmetric, with a dihedral V2−V8−V4−V6 angle of 28° (B3LYP) or 38° (BP86). The V6 atom remains unsaturated. When V6 forms an additional bond to O13, a much more stable and symmetric (D_{2h}) structure, **4-SQUARE** is obtained (vide infra). However, to make such a ring closure possible, the O9 atom must move to the opposite side of the V6−O5−V4−O7 plane. Since this costs energy, the **ONE-BRIDGE** structure exists as a local minimum stabilized by repulsion between the O9 and O13 atoms which point against each other.

The **DOUBLE-BRIDGE** cluster results from the optimization of a crystal fragment cut from the crystal along the *B* axis. The *trans* configuration shown in Figure 4 is slightly (6.7 kJ/mol, BP86) more stable than a *cis* structure, but the latter is not a minimum. The **DOUBLE-BRIDGE** structure contains two 4-fold and two triply coordinated vanadium atoms.

A cut along the *B* crystal axis, after optimization, yields the **4-RIBBON** structure (Figure 4). Its most distinctive feature is the preservation of two triply coordinated oxygen atoms O4 and O11. The $V-O^{bridging}$ bonds are considerably elongated compared to the V_2O_5 cluster, but still shorter than in the bulk structure. The V2−O4 and V12−O11 bonds remain rather short. Although the metal atom environment has become tetrahedral and thus bond angles differ considerably from the bulk values, and the entire structure is rather puckered, the **4-RIBBON** cluster exhibits the most similarity with a crystal structure fragment among all the V_4O_{10} structures considered.

Next, we generate starting structures by combining two V_2O_5 units ("synthetic approach"). Within this approach the **4-DOUBLE-BRIDGE** cluster can be built by connecting two singly bridged VO_2-O-VO_2 molecules. The **4-RIBBON** structure can be created from two V_2O_5 units if the bridging O4 atoms of each unit are connected with the V2 atoms of the other. Connecting the O7 atom of one V_2O_5 moiety to the V6 atom

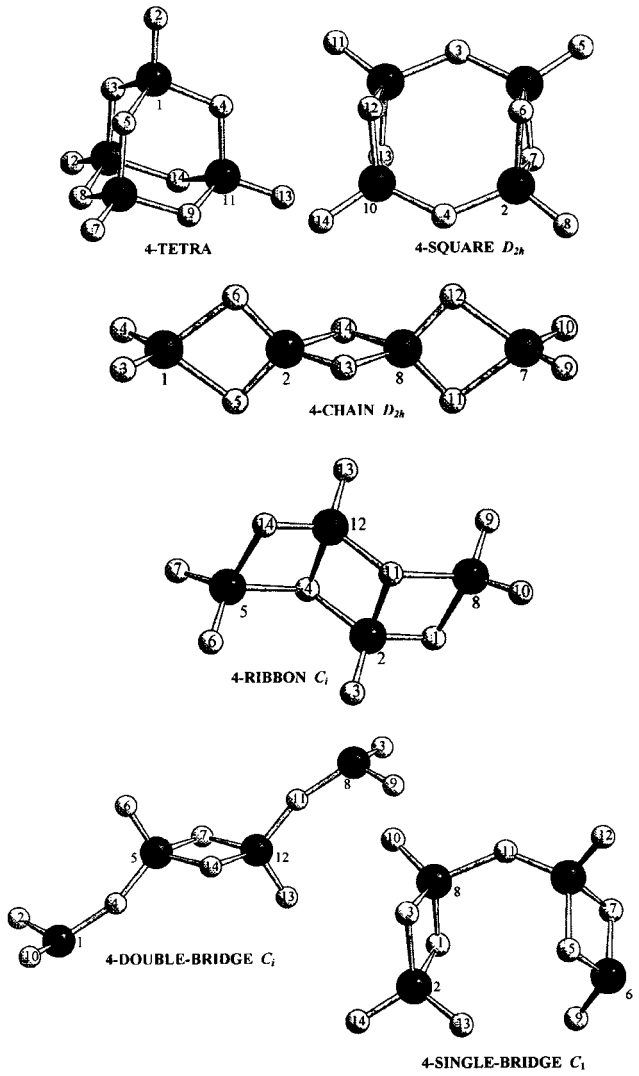

Figure 4. DFT optimized structures of various isomers of the V_4O_{10} molecule.

of the other results in a linear arrangement of the four metal atoms which are pairwise connected by double oxygen bridges. We refer to this structure as **4-CHAIN** (Figure 4). The optimized geometry has D_{2h} symmetry. Assuming that the four terminal V═O bonds are double bonds and the central bridging V−O bonds are single bonds, the valence of 5 for V and the valence of 2 for O implies bond orders of 1.5 for the V2−O6, V2−O5, V8−O11, and V8−O12 bonds as well as bond orders of 0.5 for the V1−O6, V1−O5, V7−O12, and V7−O11 bonds. The calculated bond distances follow this bond order scheme.

Another combination mode connects a terminal oxygen O2 or O3 of one V_2O_5 moiety to the (formally unsaturated) triply coordinated vanadium V6 of the other moiety, and vice versa. This procedure creates a ring with two doubly bridged opposite sides and two other singly bridged sides. The optimization of this isomer leads to a planar arrangement of vanadium atoms (D_{2h} symmetry), **4-SQUARE**, already mentioned above (Figure 4). All four vanadium atoms are tetrahedrally coordinated, each of them has one short (terminal) and three longer (bridging) bonds. The two types of $V-O^{bridging}$ bonds (singly and doubly bridging) have almost the same length.

There may be clusters that can be generated neither by the "analytic" nor by the "synthetic" approach. Since V_4O_{10} is iso-(valence)electronic with the tetraphosphorus decaoxide molecule, P_4O_{10}, in which the phosphorus atoms form a perfect

tetrahedron, an analogous structure for V_4O_{10} should be considered. Its optimization results in a very stable tetrahedral structure **4-TETRA** (see Figure 4), which has a pronounced closed-cage character. There are terminal V═O double bonds (about 160 pm) and bridging V−O single bonds (about 180 pm). (BP86 predicts slightly longer V−O bond length than B3LYP, but the difference does not exceed 2 pm.)

The **4-TETRA** structure is the most stable V_4O_{10} isomer. Relative to two V_2O_5 units, the energy is about −600 kJ/mol, a marked stabilization gained by the cage formation. The **4-SQUARE** cluster is only 15 kJ/mol $VO_{2.5}$ less stable than **4-TETRA**. In both of these isomers all metal atoms are tetrahedrally coordinated, all V atoms are pentavalent, and all O atoms are bivalent. The other isomers are substantially higher in energy. Third in stability is **4-CHAIN**, which is about 60 and 45 kJ/mol $VO_{2.5}$ above **TETRA** and **4-SQUARE**, respectively. The only structure that contains triply coordinated oxygen atoms, **4-RIBBON**, is about 70 kJ/mol $VO_{2.5}$ less favorable than **4-TETRA**. The **4-SINGLE-BRIDGE** and **4-DOUBLE-BRIDGE** structures which have triply coordinated metal atoms are even higher in energy.

4.3. V_8O_{20} Clusters. Figure 5 shows the optimized and some of the initial structures for the V_8O_{20} clusters. Following the "analytic" approach, we cut such fragments out of the crystal that would generate the entire periodic structure by translations. One possibility is to cut a fragment from two ribbons of one layer of the bulk structure. This structure, **8-Y-0** (Figure 5), contains metal atoms with coordination numbers 3 to 5 and oxygen atoms with coordination numbers between 1 (terminal) and 2 or 3 (bridging). In the course of optimization, the structure changed significantly to yield the cluster **8-SHEET-1** (Figure 5). First, all but one (O17) of the triply coordinated oxygen atoms gave up one bond to adopt a double coordination. Second, all pentacoordinated V atoms lose the fifth coordination and form a tetrahedral environment. The only exception is V14, which remains triply coordinated. The **8-SHEET-1** structure is not symmetric. However, symmetry could be restored by creating an identical environment on the left- and right-hand side with respect to the O7−O20 line. This can be done in two ways. One can remove the triply coordination of the O17 atom by breaking the V4−O17 bond. Alternatively, one can saturate the triply coordinated V14 atom by linking it to the O11 atom. In doing so, two other starting structures are generated. Their optimization yields the clusters **8-SHEET-2** and **8-SHEET-3**. They are by 62 kJ/mol less stable and 49 kJ/mol more stable than **SHEET-1**, respectively. Another structure, which is very similar to **SHEET-3** and differs from it only in topology, **SHEET-4** (Figure 5), is only 6 kJ/mol higher in energy than **SHEET-3**. Another two-dimensional structure presented in Figure 5, **SHEET-5,** is 23 kJ/mol more stable than **SHEET-3**. It is the smallest cluster in this work with pentacoordinated vanadium atoms. It should be noted, however, that the trigonal-pyramidal coordination is not typical of vanadium (V). Moreover, the V9−O3 and V9−O7 bonds are quite long (about 210−220 pm).

If a V_8O_{20} fragment is cut from one chain of a V_2O_5 layer of the crystal, the **8-X-0** structure is obtained (Figure 5), which can be alternatively generated by linking two V_4O_{10} **4-RIBBON** clusters together. The cluster of C_i symmetry resulting from the optimization of this structure is **8-RIBBON**. Compared to the initial struture, both pentacoordinated metal atoms lost the fifth bond to become tetrahedrally coordinated. Correspondingly, only two oxygen atoms remain triply coordinated. The structure is rather puckered.

8-POLYCYCLE-1 (Figure 5) is one of two additional isomers with a nearly planar arrangement of the metal atoms. It resembles the **4-SQUARE** structure, but has four penta-coordinated tetragonal−pyramidal vanadium atoms. Energetically, it lies 6 kJ/mol above the least stable "sheet" cluster, **8-SHEET-2**. **8-POLYCYCLE-2,** unlike **8-POLYCYCLE-1** preserves the tetrahedral environment of the metal atoms. There are no triply coordinated oxygen atoms in these structures.

A nonplanar cluster is obtained by cutting a fragment from two layers of the periodic structure (**8-Z-0**, Figure 5). The initial structure consists of two V_4O_{10} fragments (**4-RIBBON**) placed over each other. Optimization changes the structure very strongly (**8-TWO-LAYER-1**, Figure 5). The weak interlayer V···O interactions turned into normal V−O bonds. The longest of these, V10−O15, is 191 pm. One of the metal atoms (V18) remains pentacoordinated and only two of the oxygen atoms (O4 and O25) remain triply coordinated. A similar, but by 108 kJ/mol more stable structure is **8-TWO-LAYER-2**.

Since a cage structure (**4-TETRA**) was found to be the most stable of the V_4O_{10} clusters, an analogous cubelike V_8O_{20} isomer may be very important. The corresponding optimized cluster **CUBE** has S_4 symmetry (Figure 5) and is by far the most stable (Table 5) among the 11 V_8O_{20} clusters considered. It is followed by the **8-TWO-LAYER-2** isomer which is the only isomer besides **CUBE** in which all vanadium atoms are tetrahedrally coordinated, and no triply coordinated oxygen atoms are present. Next in stability are **8-TWO-LAYER-1** and **8-RIBBON-1** cluster, which is the most stable two-dimensional sheetlike structure. Among the true "sheet" clusters **8-SHEET-1** to **8-SHEET-5**, **8-SHEET-5** is the most stable. Since this structure features pentacoordinated vanadium atoms, one can conclude that pentacoordinated vanadium is no longer so unfavorable in V_8O_{20} as it is in V_4O_{10} clusters.

4.4. $V_{16}O_{40}$ Clusters. For species of such size the basis set used, D(T)ZVP, consists of 1144 basis functions. This makes it very costly to examine a broad range of such clusters. Therefore, we consider a small set of $V_{16}O_{40}$ structures that are of particular interest with respect to comparison with the most stable isomers of smaller clusters and the periodic bulk structure. We use $V_{16}O_{40}$ fragments cut out of the periodic divanadium pentaoxide structure along the *A*, *B*, or *C* crystal axes, **16-X-0**, **16-Y-0**, and **16-Z-0**, respectively, as initial structures for geometry optimizations (Figure 6). The **16-X-0** fragment consists of two ribbons of one layer of the periodic structure. It has nine pentacoordinated, six tetracoordinated, and one triply coordinated metal atoms. The cluster obtained after optimization **16-DOUBLE RIBBON**, retains the main features of the initial structure, although the coordination of some of the atoms has changed. Five metal atoms in the middle of the cluster preserved their 5-fold coordination, and only those at the boundary adopted a tetrahedral environment. The structure found is probably only one of several "sheetlike" $V_{16}O_{40}$ clusters with slightly different coordinations. The **16-Y-0** fragment (Figure 6) is also "sheet-like", but made of four ribbons of one crystal layer. The structure resulting after optimization **16-SHEET** retains the overall "sheetlike" structure and only atoms at the clusters boundary assume a different coordination.

The two-layer fragment considered **16-Z-0** is a stack of two V_8O_{20} "sheet" fragments similar to **8-Y-0** (Figure 6). Optimization converts it into a double-layer structure **16-TWO-LAYER**, in which only tetrahedrally coordinated vanadium atoms and, besides terminal V═O bonds, only doubly coordinated oxygen bridges are present. A closer inspection shows that this structure has the topology of a octagonal prism with 16 $V{=}O(O-)_{3/2}$

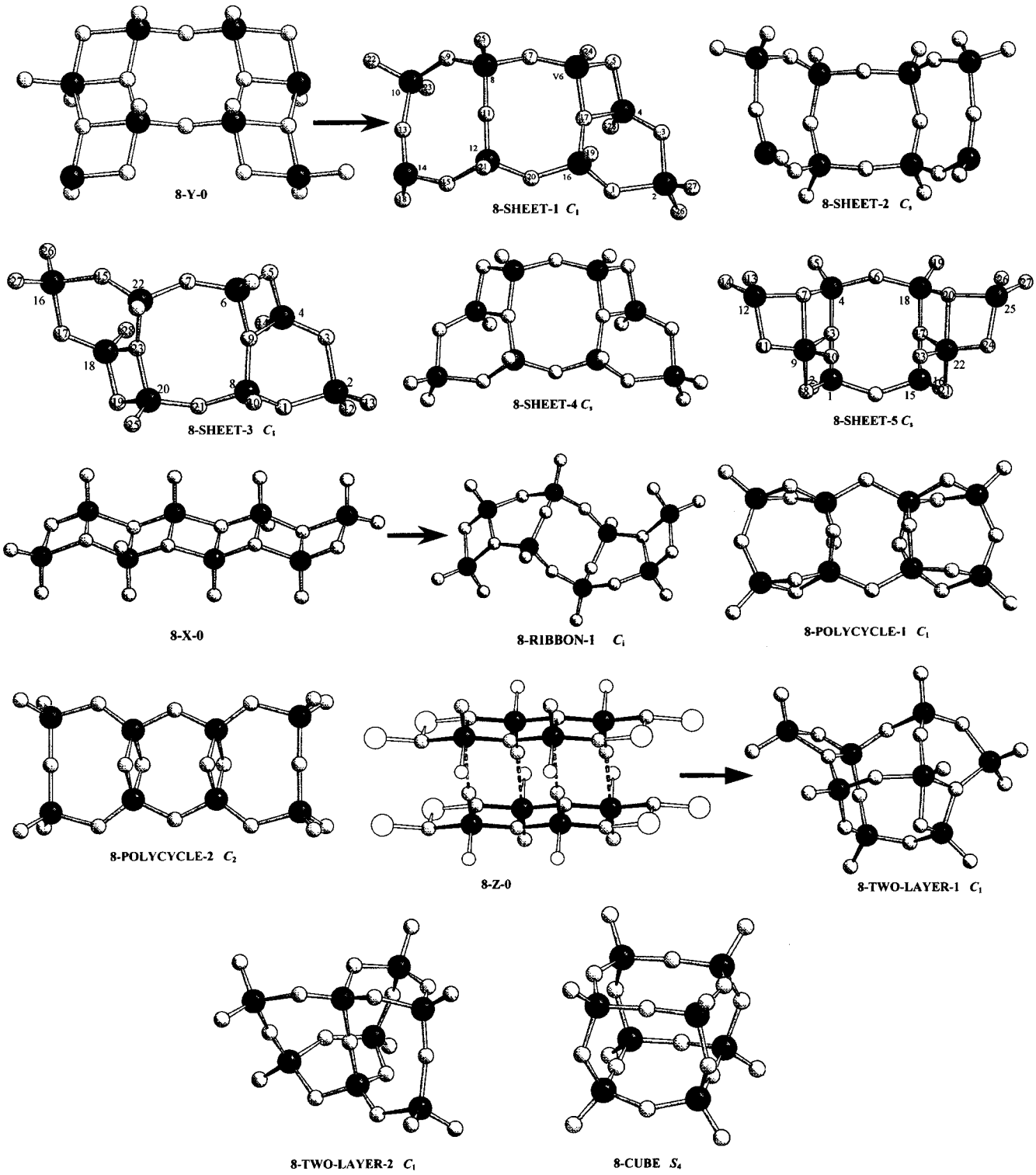

Figure 5. BP86/D(T)ZVP optimized structures of V_8O_{20} clusters. The arrows connect initial and resulting (optimized) structures.

units as apexes. However, compared to this perfect cage, the structure found has a "defect".

In one of the octagons which form the upper and lower faces of the prism a pair of neighbored $V{=}O(O{-})_{3/2}$ units is replaced by one $V{=}O(O{-})_{4/2}$ and one $V{=}O(O{-})_{2/2}$ unit. Thus, instead of an octagon with an adjacent square in the perfect cage, we have a heptagon with an adjacent pentagon in the **16-TWO-LAYER** structure. Otherwise, the topology persists.

Upon optimizing the perfect octagonal prism of $V{=}O(O{-})_{3/2}$ units, the **16-OCT-PRISM** structure is obtained (Figure 6). Its main difference to **16-TWO-LAYER** is that all terminal oxygen atoms are directed outward, while in **16-TWO-LAYER** the V−O bonds partly inherited a nearly collinear arrangement. This outward direction of the V═O bonds reduces steric hindrance and, hence, lowers the energy by about 8 kJ/mol $VO_{2.5}$.

The energies of the four $V_{16}O_{40}$ isomers differ substantially. The **16-DOUBLE-RIBBON** cluster is not particularly stable, comparable in stability with the V_8O_{20} clusters **8-RIBBON** and **8-SHEET-5**. The other "sheet"-type cluster **16-SHEET** is more stable than **16-DOUBLE-RIBBON** and also than **8-SHEET-5**. In agreement with our findings for the V_8O_{20} clusters, the

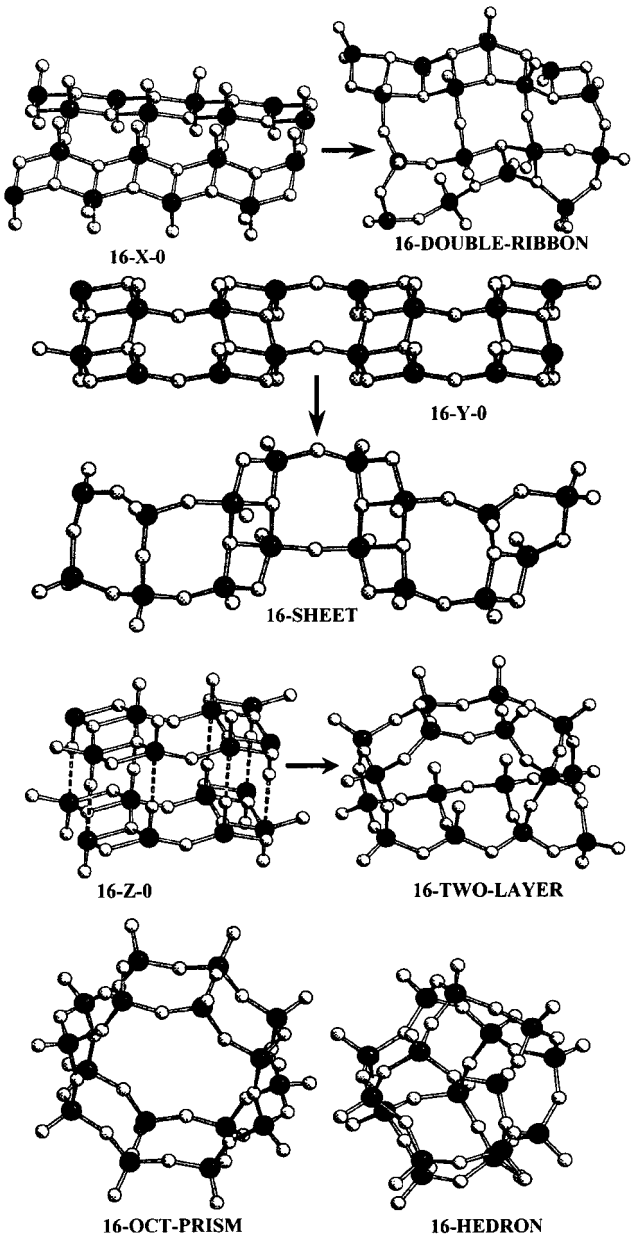

Figure 6. BP86/D(T)ZVP optimized structures of $V_{16}O_{40}$ clusters. The arrows connect initial and resulting (optimized) structures.

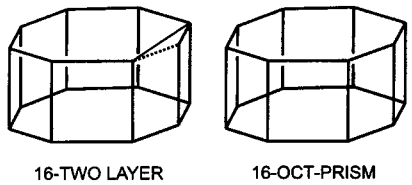

Figure 7. Cage-type structures of **OCT-PRISM** and **16-TWO-LAYER** clusters. The apexes of the polyhedrons represent vanadyl (V═O) groups; edges are V−O−V bridges.

16-TWO-LAYER cluster is much more stable than the "sheet" clusters, but still less stable than V_8O_{20} **CUBE**. Only the most stable of the four $V_{16}O_{40}$ clusters considered, **OCT-PRISM**, is more stable than the most stable V_8O_{20} cluster, **CUBE.**

4.5. Cage-Type Clusters of Various Size. The most stable isomers of $(VO_{2.5})_n$ clusters with $n = 4$, 8, and 16 found all are regular polyhedra of V═O(O−)$_{3/2}$ units: tetrahedron, cube, and octagonal prism (Figures 7, 8). These polyhedra have V═O units at the apexes and bridging O atoms on the edges. This principle

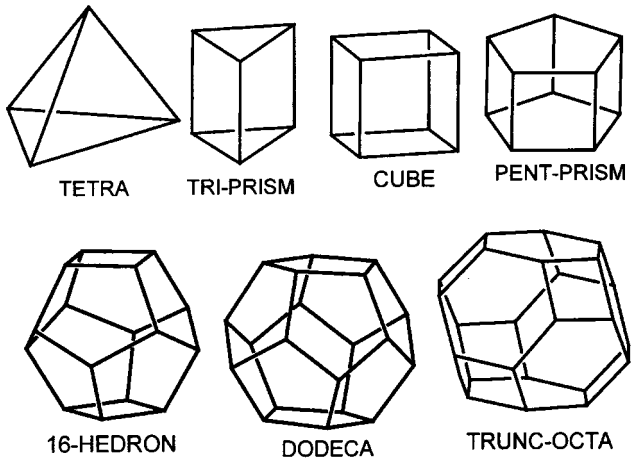

Figure 8. Cage-type structures of $(V_2O_5)_n$ clusters ($n = 2$, 3, 4, 5, 8, 10, and 12). The apexes of the polyhedrons represents vanadyl (V═O) groups, edges are V−O−V bridges.

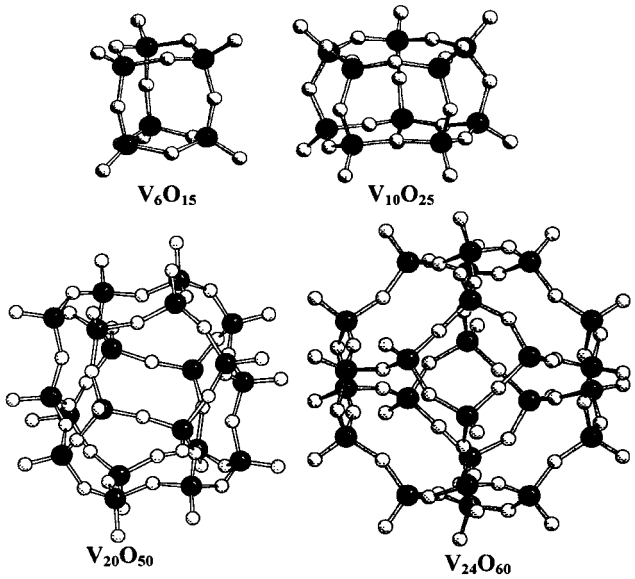

Figure 9. BP86/D(T)ZVP optimized structures of V_6O_{10}, $V_{10}O_{25}$, $V_{20}O_{50}$, and $V_{24}O_{60}$ cage clusters.

suggests that for all cluster sizes from $n = 4$ to an unknown limit the most stable structures are spherical with the V═O-(O−)$_{3/2}$ groups forming regular polyhedra.[55] Hence, for $n = 6$ and $n = 10$, the trigonal and pentagonal prisms, respectively (double three- and five-membered rings, respectively) are possible candidates for the most stable isomers of $(VO_{2.5})_n$ clusters. For $n = 16$, in addition to the octagonal prism already examined, another 16-hedron with eight pentagons and two squares as faces could be more stable because it is more spherical than the octagonal prism. For $n = 20$ the pentagon−dodecahedron (all 12 faces are pentagons) and for $n = 24$ the truncated octahedron (eight faces are hexagons and six faces are squares) are very likely to be the most stable structures.

We have optimized these cage structures for $n = 6$, 10, 16, 20, and 24. In the minimum energy structure for $n = 6$, **TRI-PRISM** (Figure 9), the trigonal faces are six-membered rings in chair conformation, i.e., the bridging O atoms are shifted outward from the V···V line. In the energy minimum structure for $n = 10$, **PENTA-PRISM** (Figure 9), the five V atoms in the pentagonal faces are almost exactly within one plane, with three of the bridging O atoms shifted outward from the V···V lines and two of them shifted inward. For $n = 16$ the optimized

TABLE 8: IR Spectra of V_2O_5 Isomers

$OV-(O_2)-VO_2$ C_s				$O_2V-O-VO_2$ C_2			
ν, cm^{-1}	A, km/mol	symmetry		ν, cm^{-1}	A, km/mol	symmetry	
1057	137	A′	$V-O^{(1)}$-str[a]	1040	234	A	$V-O^{(1)}$-str
1038	196	A′	$V-O^{(1)}$-str	1035	212	B	$V-O^{(1)}$-str
1026	244	A′	$V-O^{(1)}$-str	1032	52	A	$V-O^{(1)}$-str
859	122	A′	sym $V-O^{(2)}$-str	1016	219	B	$V-O^{(1)}$-str
799	149	A″	as. $V-O^{(2)}$-str	876	742	B	as. $V-O^{(2)}-V$-str
537	115	A′	$O^{(2)}-V-O^{(2)}$-str	464	7	A	
413	5	A′		370	9	B	
379	7	A″		328	1	A	
352	21	A′		281	39	B	
309	2	A″		267	22	A	
260	2	A′		164	59	B	
187	9	A′		159	9	A	
164	2	A″		43	0	A	
155	24	A″		38	13	B	
72	7	A′		26	8	A	

[a] str = stretch. sym = symmetry. as. = asymmetry.

16-hedron structure does not have symmetry. It is about 2 kJ/mol $VO_{2.5}$ more stable than the **OCT-PRISM**. For $n = 20$, optimization yielded a slightly distorted dodecahedron of D_{3d} symmetry, **DODECA** (Figure 9). The perfect structure of I_h symmetry, which requires almost linear V−O−V bridges, is about 17 kJ/mol $VO_{2.5}$ higher in energy. The optimization of the truncated octahedron ($n = 24$) converges toward a structure of T_d symmetry shown in Figure 9 (the starting structure had T symmetry). When the symmetry was constrained to T_d the energy did not increase. Moreover, a fully unconstrained (C_1) optimization starting from a slightly distorted structure resulted in the same structure. Hence, the T_d structure was accepted as the lowest energy structure. As expected, the relative energies of the V_6O_{15} and $V_{10}O_{25}$ clusters are intermediate between V_4O_{10} and V_8O_{20}, and between V_8O_{20} and $V_{16}O_{40}$, respectively. Therefore, in the series of the most stable isomers (all are cage structures) **4-TETRA**, **6-TRI-PRISM**, **8-CUBE 10-PENT-PRISM**, **16-hedron**, **DODECAhedron**, and **TRUNC-OCT** the energy per $VO_{2.5}$ unit decreases monotonically with increasing cluster size (Table 5).

5. Discussion

5.1. Structures. From $n = 2$ on, the most stable isomers of $(V_2O_5)_n$ clusters are polyhedral cages with vanadyl groups, V═O, at the apexes and bridging oxygen atoms on the edges. Hence, vanadium is always 4-fold coordinated and pentavalent while oxygen is always divalent. This is qualitatively different from the structure of the bulk V_2O_5 crystal, which also features 3-fold coordinated oxygen atoms and in which all vanadium atoms are coordinated to five oxygen atoms within one layer with an additional weak sixth coordination to vanadyl groups of the next layer.

The polyhedral structures of the $(V_2O_5)_n$ gas-phase clusters follow a general structure principle for spherical molecular hosts for which many examples exist in inorganic and organic chemistry.[55] This is the same building principle as found for anionic silicate species in solution, $[SiO^-(O-)_{3/2}]$,[56] or for polyhedral building units in framework silicates, $[Si(O-)_{4/2}]$.[57] For example, the trigonal prism and the cube have been identified by NMR techniques[56] in silicate solutions. In the structural chemistry of zeolites the hexagonal prism and the truncated octahedron are found in faujasite. The latter is also known as β-cage or sodalite cage.[57]

In solution, complex vanadate anions with all vanadium atoms in the formal oxidation state V^V do exist. They are related to the neutral clusters studied here by the formal process

$$(V_2O_5)_n + mH_2O \rightarrow H_xV_{2n}O_{5n+m}^{(2m-x)-} + (2m - x)H^+$$

Examples are the $V_{12}O_{32}^{4-}$ [58] and the $V_{10}O_{28}^{6-}/H_3V_{10}O_{28}^{3-}$ ions.[59] The structures of salts containing such oxygen rich anions have been determined by X-ray diffraction.[58,59] In the presence of suitable template molecules or ions, they may assume the shape of bowls[59] or cages.[60] The latter have so far only be observed with mixed valent V^VV^{IV} oxide anions.[60] As the bulk V_2O_5 solid these complex vanadate anions have 3-fold coordinated oxygen atoms and 5-fold coordinated vanadium atoms. However, they contain more oxygen atoms per vanadium than the neutral gas-phase species considered in this study. The structure of some other vanadate(V) ions[61] resembles some of the less stable isomers of gas-phase clusters. For example, the metavanadate $(VO_3^-)_\infty$ ion is built similarly to our **4-CHAIN** isomer, and the cyclic $V_4O_{12}^{4-}$ ion resembles remotely our **4-SQUARE** isomer. It has tetrahedrally coordinated vanadium atoms but only single oxygen bridges.

5.2. Vibrational Spectra. Neutral clusters of $(V_2O_5)_n$ composition have not yet been studied in the gas phase. However, advances in IR laser spectroscopy due to the free eletron laser technique render such studies possible. Recently, von Helden et al. observed the infrared spectra of gas-phase zirconium oxide clusters.[4] Guided by predicted IR spectra, inferences about the structure of the clusters are possible. For some of the cluster structures predicted in this study we have calculated the IR spectra in harmonic approximation using the BP86 functional. The characteristic bands obtained for different stretching vibrations involving differently coordinated oxygen atoms fit to the bands observed for polycrystalline V_2O_5 samples:[62] 1023 and 982 cm^{-1} ($V═O^{(1)}$), 813 cm^{-1} ($V-O^{(2)}$), as well as 605 and 472 cm^{-1} ($V-O^{(3)}$).

Table 8 shows the vibrational frequencies and IR intensities for the two V_2O_5 isomers. The different number of terminal V═O bonds in the single bridge and double bridge structures gives rise to three and four bands, respectively, in the $V═O^{(1)}$ stretching region above 1000 cm^{-1}. Nevertheless, discrimination based on this feature will not be easy because of the very small splittings predicted between bands in the $O_2V-O-VO_2$ isomer. The $V-O^{(2)}-V$ stretching region is better suited. It shows three about equally intense bands between 925 and 500 cm^{-1} for the more stable $OV-(O_2)-VO_2$ isomer, but only one very intense band at 876 cm^{-1} for the less stable $O_2V-O-VO_2$ isomer.

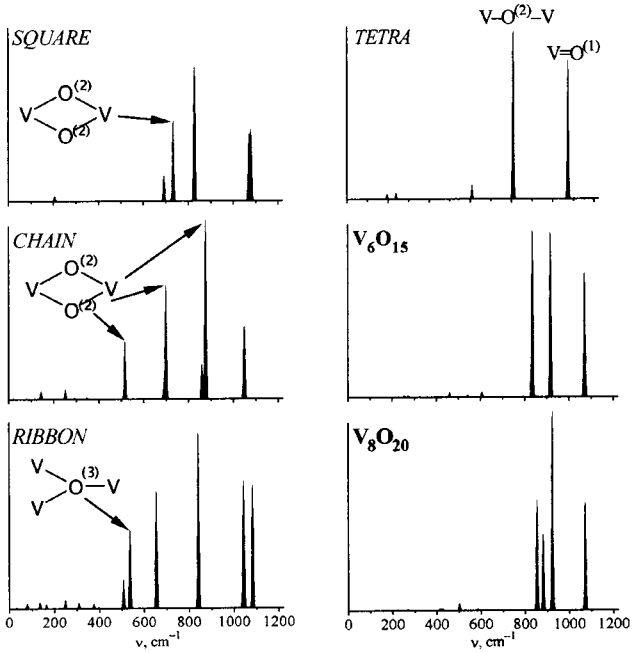

Figure 10. IR spectra of diferent V_4O_{10} isomers (left) and cage-type clusters of different size (right).

Figure 10 shows the predicted IR spectra for different V_4O_{10} isomers and for the most stable cage-type structures of V_6O_{15} and V_8O_{20}. Characteristic of the most stable cage-type structures are the $V{=}O^{(1)}$ stretching and the asymmetric $V{-}O^{(2)}{-}V$ stretching bands in the regions between 1040 and 1080 cm^{-1} and 800−925 cm^{-1}, respectively. Depending on the symmetry, there may be one or more bands in these regions. The less stable **SQUARE** isomer of V_4O_{10} is distinguished from the **TETRA** cage structure by a doublet of bands around 700 cm^{-1} which are due to the $V{-}O_2^{(2)}{-}V$ double bridge. Three such double bridges with different bond length are characteristic of the **CHAIN** isomer. Correspondingly, there are three different bands at 876, 699, and 516 cm^{-1}. The **RIBBON** structure which is the only one preserving triply coordinated oxygen as a characteristic motif of the structure of the bulk solid shows a very similar band pattern. The only difference is that the absorption at 536 cm^{-1} is now due to $V{-}O^{(3)}$ stretch vibrations involving the triply coordinated oxygen.

Hence, the most stable cage-type structures with only two types of oxygen atoms, terminal $V{=}O^{(1)}$ and bridging $V{-}O^{(2)}{-}V$, could be identified by IR spectra showing bands in the 1040−1080 cm^{-1} and in the 800−925 cm^{-1} regions, but not between 650 and 750 cm^{-1} or around 500 cm^{-1}. The latter are characteristic of $V{-}O_2(2){-}V$ double bridges or triply coordinated oxygen. Vibrational frequencies calculated at the level of approximation adopted here (BP86 functional, harmonic approximation) may deviate from the observed values by one to several percent. For example, based on a large number of nontransition metal molecules, a scaling factor of 0.9914 was proposed to improve BP86 frequencies.[63]

5.3. Stability. The stability of the cage-type clusters increases monotonically with increasing size. The energy difference between the largest cluster studied ($n = 24$) and the bulk solid (Table 5) is only 3 kJ/mol, on the order of the interlayer binding in the bulk solid. The predicted stability difference between gas-phase clusters and the bulk solid may be affected by the inherent error connected with the computational technique used. A different calculation also based on DFT, but using another functional (Perdew-Wang), a plane wave basis set and a pseudopotential for the core electrons, predicts that the **TETRA** cluster is by 53 kJ/mol $VO_{2.5}$ less stable than the periodic bulk structure[64] compared to 41 kJ/mol $VO_{2.5}$ found in this study.

For the V_4O_{10} gas-phase species an estimate of thermochemical data is available, albeit with a large uncertainty. The heat of formation determined at 1104 K and extrapolated to 298 K using estimated temperature coefficients, $\Delta_f H^o_{298}$ ($V_4O_{10,g}$) = −2866 kJ/mol,[65] combined with the data for solid V_2O_5, $\Delta_f H^o_{298}$ ($V_2O_{5,s}$) = −1551 kJ/mol[66] yields an estimate for the reaction enthalpy of the following hypothetical process:

$$\frac{1}{2}\{V_2O_5\}_s \rightarrow \frac{1}{4}\{V_4O_{10}\}_g$$

The result, $\Delta_R H^\circ_{298} = 59$ kJ/mol $VO_{2.5}$, is close to our predicted reaction energy of 41 kJ/mol $VO_{2.5}$ and even closer to the plane wave-pseudopotential result just mentioned, 53 kJ/mol $VO_{2.5}$.

6. Conclusions

(1) The structures of $(V_2O_5)_n$ gas-phase clusters are very different from the layer structure of the solid bulk. Instead of a 6-fold coordination in the crystal structure vanadium tends to adopt a 4-fold coordination with one terminal V=O and three bridging V−O bonds in gas phase clusters. Contrary to the crystal structure, triply coordinated oxygen atoms are avoided, unless this is necessary to saturate vanadium which otherwise would have coordination numbers less than four. Cluster structures that correspond to fragments cut out of the crystal structure are very high in energy.

(2) Starting from $2n = 4$, the most stable isomers are polyhedral cages with vanadyl groups, V=O, at the corners and bridging oxygen atoms on the edges. This is the same structure type as found, e.g., for anionic silicate species in solutions or in building units of framework silicates.

(3) The energies of the most stable clusters per formula unit decrease monotonically with increasing cluster size. The energies of the largest clusters studied, $2n = 16$, 20 and 24, are above that of the bulk solid by about 3−5 kJ/mol $VO_{2.5}$ only. This difference is on the order of the interlayer binding in solid V_2O_5.

(4) Experimental information about the $(V_2O_5)_n$ gas-phase clusters can be obtained by IR spectroscopy. The most stable cage-type structures should show bands in the 1040−1080 cm^{-1} (terminal $V{=}O^{(1)}$) and 800−925 cm^{-1} regions (bridging $V{-}O^{(2)}{-}V$), but not between 650 and 750 cm^{-1} ($V{-}O_2^{(2)}{-}V$ double bridges) or around 500 cm^{-1} (triply coordinated oxygen).

Acknowledgment. This work has been supported by the Deutsche Forschungsgemeinschaft within the Sonderforschungsbereich 546, by the Max-Planck-Gesellschaft, and by the Fonds der Chemischen Industrie. Computer time provided by the Konrad-Zuse-Zentrum für Informationstechnik Berlin (CRAY T3E) is also appreciated.

Supporting Information Available: Absolute energies of vanadium oxide clusters and bulk solid as well as those of vanadium and oxygen atoms. This material is available free of charge via the Internet at http://pubs.acs.org.

References and Notes

(1) Castleman, A. W., Jr.; Bowen, K. H. *J. Phys. Chem.* **1996**, *100*, 12911.

(2) Guo, B. C.; Kerns, K. P.; Castleman, A. W., Jr. *Int. J. Mass Spectrom. Ion Processes* **1992**, *117*, 129.

(3) Deng, H. T.; Kerns, K. P.; Castleman A. W., Jr. *J. Phys. Chem.* **1996**, *100*, 13386.

(4) von Helden, G.; Kirilyuk, A.; van Heijnsbergen, D.; Sartakov, B.; Duncan, M. A.; Meijer, G. *Chem. Phys.* **2000**, *262*, 31.
(5) Ahlrichs, R.; Ochsenfeld, Ch. *Ber. Bunsen-Ges. Phys. Chem.* **1992**, *96*, 1287.
(6) Ochsenfeld, Ch.; Ahlrichs, R. *J. Chem. Phys.* **1992**, *98*, 34.
(7) Ochsenfeld, Ch.; Ahlrichs, R. *J. Chem. Phys.* **1992**, *97*, 3487.
(8) Aguado, A.; López, J. M. *J. Phys. Chem. B*, **2000**, *104*, 8398.
(9) Kung, H. H. *Transition Metal Oxides, Surface Chemistry and Catalysis*; Elsevier: New York, 1989.
(10) Haggin, J. *Chem. Eng. News* **1995**, *73*, 20.
(11) Topsøe, N.-Y. *Science* **1994**, *265*, 1217.
(12) Bachmann, H. G.; Ahmed, F. R.; Barnes, W. H. *Z. Kristallogr., Kristallgeom., Kristallphys., Kristallchem.* **1961**, *115*, 110.
(13) Bell, R. C.; Zemski, K. A.; Kerns, K. P.; Deng, H. T.; Castleman, A. W., Jr. *J. Phys. Chem. A* **1998**, *102*, 1733.
(14) Kooi, S. E.; Castleman, A. W., Jr. *J. Phys. Chem. A* **1999,** *103*, 5671.
(15) Bell, R. C.; Zemski, K. A.; Castleman, A. W., Jr. *J. Phys. Chem. A* **1999**, *103*, 2992.
(16) Bell, R. C.; Zemski, K. A.; Castleman, A. W., Jr. *J. Phys. Chem. A* **1999**, *103*, 1585.
(17) Harvey, J.; Diefenbach, M.; Schröder, D.; Schwarz, H. *Int. J. Mass Spectrom.* **1999**, *182/183*, 85.
(18) Rudnyi, E. B.; Kaibicheva, E. A.; Sidorov, L. N. *J. Chem. Thermodyn.* **1993**, *25*, 929.
(19) Dinca, A.; Davis, Th.P.; Fisher, K. J.; Smith, D. R.; Willett, G. D. *Int. J. Mass Spectrom.* **1999**, *182/183*, 73.
(20) Rademann, K.; Pramann, A. Private communication. Humboldt-Universitat Berlin, 1999.
(21) Wu, H.; Wang, L.-S. *J. Chem. Phys.* **1998**, *108*, 5310.
(22) Foltin, M.; Stueber, G. J.; Bernstein, E. R. *J. Chem. Phys.* **1999**, *111*, 9577.
(23) Vyboishchikov, S. F.; Sauer, J. *J. Phys. Chem. A* **2000**, *104*, 10913.
(24) Kempf, J. Y.; Silvi, B.; Dietrich, A.; Catlow, C. R. A.; Maigret, B. *Chem. Mater.* **1993**, *5*, 641.
(25) Lambrecht, W.; Djafari-Rouhani, B.; Lannoo, M.; Vennik, J. *J. Phys. C* **1980**, *13*, 2485.
(26) Fiermans, L.; Clauws, P.; Lambrecht, W.; Vandenbroucke, L.; Vennik, J. *Phys. Status Solidi A* **1980**, *59*, 485.
(27) Bullett, D. W. *J. Phys. C.* **1980,** *13*, 1595.
(28) Parker, J. C.; Lam, D. J.; Xu, Y.-N.; Ching, W. Y. *Phys. Rev. B* **1996**, 42, 5289.
(29) Eyert, V. In *Density-Functional Methods: Applications in Chemistry*; Springborg, M., Ed.; Wiley: Chichester, 1997.
(30) Eyert, V.; Hock, K.-H. *Phys. Rev. B* **1998**, *57*, 12727.
(31) Chakrabarti, A.; Hermann, K.; Druzinic, R.; Witko, M.; Wagner, F.; Petersen, M. *Phys. Rev. B* **1999**, *59*, 10583.
(32) Yin, X.; Fahmi, A.; Endou, A.; Ryuiji, M.; Gunji, I.; Yamauchi, R.; Kubo, M.; Chatterjee, A.; Miyamoto, A. *Appl. Surf. Sci.* **1998**, *130*−*132*, 539.
(33) Parr, R. G.; Yang, W. *Density Functional Theory of Atoms and Molecules*; Oxford University Press: New York, 1989.
(34) Becke, A. D. *J. Chem. Phys.* **1993**, *98*, 5648.
(35) Stephens, P. J.; Devlin, C. F.; Chabalowski, M. J.; Frisch, M. J. *J. Phys. Chem.* **1994**, *98*, 11623.
(36) Becke, A. D. *Phys. Rev. A* **1988**, *38*, 3098.
(37) Lee, C.; Yang, W.; Parr, R. G. *Phys. Rev. B* **1988**, *37*, 785.
(38) Perdew, B. P. *Phys. Rev. B* **1986**, *B33*, 8822.
(39) Koch, W.; Hertwig, R. In *Encyclopedia of Computational Chemistry*; Schleyer, P. v. R., Ed.; John Willey & Sons: Chichester, 1998; Vol. 1, 689−700.
(40) Görling, A.; Trickey, S. B.; Gisdakis, P.; Rösch, N. *Top. Organomet. Chem.* **1999**, *4*, 109.
(41) Ahlrichs, R.; Furche, F.; Grimme, S. *Chem. Phys. Lett.* **2000**, *325*, 317.
(42) Eichkorn, K.; Treutler, O.; Öhm, H.; Häser, M.; Ahlrichs, R. *Chem. Phys. Lett.* **1995**, *240*, 283.
(43) Schäfer, A.; Horn, H.; Ahlrichs, R. *J. Chem. Phys.* **1994**, *100*, 5829.
(44) Wachters, A. J. H. *J. Chem. Phys.* **1970**, *52*, 1033.
(45) Frisch, M. J.; Trucks, G. W.; Schlegel, H. B.; Gill, P. M. W.; Johnson, B. G.; Robb, M. A.; Cheeseman, J. R.; Keith, T.; Petersson, G. A.; Montgomery, J. A.; Raghavachari, K.; Al-Laham, M. A.; Zakrzewski, V. G.; Ortiz, J. V.; Foresman, J. B.; Cioslowski, J.; Stefanov, B. B.; Nanayakkara, A.; Challacombe, M.; Peng, C. Y.; Ayala, P. Y.; Chen, W.; Wong, M. W.; Andres, J. L.; Replogle, E. S.; Gomperts, R.; Martin, R. L.; Fox, D. J.; Binkley, J. S.; Defrees, D. J.; Baker, J.; Stewart, J. P.; Head-Gordon, M.; Gonzalez, C.; Pople, J. A. *Gaussian 94*, revision B.3; Gaussian, Inc.: Pittsburgh, PA, 1995.
(46) Ahlrichs, R.; Bär, M.; Häser, M.; Horn, H.; Kölmel, C. M. *Chem. Phys. Lett.* **1989**, *162*, 165; *Program TURBOMOLE*. TURBOMOLE is commercially available from MSI: San Diego, CA.
(47) Treutler, O.; Ahlrichs, R. *J. Chem. Phys.* **1995**, *102*, 346.
(48) Eichkorn, K.; Treutler, O.; Öhm, H.; Häser, M.; Ahlrichs, R. *Chem. Phys. Lett.* **1995**, 242, *652*.
(49) Henderson, R. A.; Hughes, D. L, Janas, Z.; Richards, R. L.; Sobota, P.; Szafert, S. *J. Organomet. Chem.* **1998**, *554*, 195.
(50) Caughan, C. N.; Smith, H. M.; Watenpaugh, K. *Inorg. Chem.* **1966**, *12*, 2131.
(51) Priebsch, W.; Rehder, D. *Inorg. Chem.* **1990**, *29*, 3013.
(52) Dovesi, R.; Saunders, V. R.; Roetti, C.; Causà, M.; Harrison, N. M.; Orlando, R.; Aprà, E. *CRYSTAL-95 User's Manual*; Università di Torino: Torino, 1996.
(53) Enjalbert, R.; Galy, J. *Acta Crystallogr. C* **1986**, *42*, 1467.
(54) Catti, M.; Sandrone, G.; Dovesi, R. *Phys. Rev. B*, **1997**, *55*, 16122.
(55) MacGillivray, L. R.; Atwood, J. L. *Angew. Chem.* **1999**, *111*, 1080; *Angew. Chem. Int. Ed.* **1999**, *38*, 1018.
(56) McCormick, A. V.; Bell, A. T. *Catal. Rev.*−*Sci. Eng.* **1989**, *31*, 97.
(57) Liebau, F. *Structural Chemistry of Silicates*; Springer: New York, 1985.
(58) Day, V. W.; Klemperer, W. G.; Yaghi, O. M. *J. Am. Chem. Soc.* **1989**, *111*, 5959.
(59) Day, V. W.; Klemperer, W. G.; Maltbie, D. J. *J. Am. Chem. Soc.* **1987**, *109*, 2991.
(60) Müller, A.; Penk, M.; Rohlfing, R.; Krickemeyer, E.; Döring, J. *Angew. Chem.* **1990**, *102*, 927; *Angew. Chem., Int. Ed. Engl.* **1990**, *29*, 926.
(61) Pope, M. T. *Heteropoly and Isopoly Oxometalates*; Springer: New York, 1983.
(62) Clauws, P.; Broeckx, J.; Vennik, J. *Phys. Status Solidi B* **1985**, *131*, 459.
(63) Scott, A. P.; Radom, L. *J. Phys. Chem.* **1996**, *100*, 16502.
(64) Brázdová, V.; Sauer, J. Unpublished paper.
(65) Hackert, A.; Gruehn, R. *Z. Anorg. Allg. Chem.* **1998**, *624*, 1756.
(66) *Handbook of Chemistry and Physics*, 81st ed.; Lide, D. R., Ed.; CRC Press: Boca Rotan, 2000.
(67) Schäfer, A.; Horn, H.; Ahlrichs, R. *J. Chem. Phys.* **1992**, *97*, 2571.